[AMERICAN JOURNAL OF SCIENCE, VOL. 276, APRIL, 1976, P. 401-424]

American Journal of Science

APRIL 1976

MINERAL REACTIONS IN PELITIC ROCKS: I. PREDICTION OF P–T–X(Fe–Mg) PHASE RELATIONS

ALAN BRUCE THOMPSON

Department Geological Sciences, Hoffman Laboratory,
Harvard University, Cambridge, Massachusetts 02138

ABSTRACT. The detailed behavior of mineral assemblages during progressive metamorphism of pelitic rocks may be predicted through P–T–X(Fe–Mg) relationships for the model system K_2O–FeO–MgO–Al_2O_3–SiO_2–H_2O. Continuous and discontinuous reactions may be examined in isobaric T–X(Fe–Mg) and isothermal P–X(Fe–Mg) sections, constructed simply from a knowledge of Mg/Fe partitioning between phases and relative dP/dT of end-member reactions in either Fe– or Mg–systems. The displacements of three-phase triangles on the AFM projection may be predicted as functions of changing pressure, temperature, or aH_2O.

INTRODUCTION

Many field and laboratory studies have been concerned with the elucidation of mineral reactions during metamorphism of pelitic rocks. Several studies have specifically dealt with the construction of a petrogenetic grid based on topological changes of the AKFM projection (J. B. Thompson, 1957) and the appropriate mineral reactions as functions of pressure (P), temperature (T), and activity of H_2O (aH_2O).

Mineral reactions in pelitic rocks have been described in terms of two complex interdependent subsystems. The first sub system, K_2O–Na_2O–(CaO)–Al_2O_3–SiO_2–H_2O (KN(C)ASH) has been considered by J. B. Thompson (1961), Evans and Guidotti (1966), A. B. Thompson (1974), and Thompson and Thompson (in preparation). The second subsystem, K_2O–(Na_2O)–MgO–FeO–Al_2O_3–SiO_2–H_2O (K(N)MFASH), has received much wider attention (see J. B. Thompson, 1957, 1972; J. B. Thompson and Norton, 1968; Albee, 1965a, b, 1972; Hoschek, 1969; Hess, 1969; Grant, 1973; and references therein).

Sufficient compositional data on coexisting minerals from various metamorphic grades as well as experimental and thermochemical data for limiting (K *or* Na with Fe *or* Mg) reactions are available to enable evaluation of general P–T–X models for metamorphism of pelitic rocks in terms of either of the above subsystems.

This study is concerned with the AFM phases — cordierite (*Crd*), chlorite (*Chl*), biotite (*Bio*), chloritoid (*Ctd*), staurolite (*Sta*), and garnet (*Gar*), coexisting with muscovite (*Mus*), K-feldspar (*Ksp*), aluminosilicates, and quartz (see table 1). The initial model was developed for assemblages low in Na_2O and CaO, although general methods have been presented for Na–Ca–K substitution in feldspars and micas (see references above). Similarly the model considers the case of unit activity of H_2O despite the

presence of carbonates, graphite, sulphides, or oxides in most pelites. A further limiting case assumes fairly constant f_{O_2} and that Fe_2O_3 can be neglected as a major component. TiO_2 is neglected as a component although it may be an important constituent of biotite, especially at higher grades.

CONTINUOUS AND DISCONTINUOUS MINERAL REACTIONS

Attempts to use the available experimental data obtained for the end-member Fe and Mg systems (KFASH and KMASH) to describe mineral reactions in pelitic rocks obviously neglect the effect of the Fe–Mg crystalline solutions. J. B. Thompson and Norton (1968) introduced the terms *simple* and *complex* to describe the types of reactions observed. These terms are synonomous with *continuous* and *discontinuous* reactions in the sense of Bowen (1928, p. 54). Thompson and Norton used the terms "simple" and "complex" to emphasize that a continuous reaction in limiting case becomes a discontinuous reaction in the end-member systems KFASH and KMASH (J. B. Thompson, personal commun., 1974).

Continuous reactions.—Reactions in the end-member systems (KFASH and KMASH) are the limiting cases of continuous reactions and may be balanced using stoichiometric coefficients appropriate to the mineral formulae presented in table 1. However, because Fe and Mg are preferentially partitioned between coexisting AFM phases, continuous reactions are in fact the resultant of two effects, one involving the Fe-components and the other Mg-components (Thompson and Norton, 1968, p. 321). These reactions involve *continuous* displacements of specific three-phase fields on an AFM diagram and would in general only be observed as a change in the relative proportions of phases in the pelitic rock, with changing metamorphic grade.

In the six-component system (KFMASH) assuming that no compositional colinearities occur between any set of three-AFM phases, there will be a *maximum* of $7!/(3! \times 4!)$ $(=35)$[1] possible continuous reactions between 3 of the 7 phases (*Crd, Chl, Bio, Ctd, Sta, Gar,* and aluminosilicate, *Als*) for *each* of the aluminosilicate phases, kaolinite (*Kao*), pyrophyllite (*Pyp*), andalusite (*And*), kyanite (*Kya*), and sillimanite (*Sil*), many of which will be metastable. For the present case, where both cordierite (*Crd*) and chloritoid (*Ctd*) have the same $(FeO+MgO)/Al_2O_3$ ratio $(=1)$, compositional degeneracies exclude five of the continuous reactions (that is, *Crd–Ctd* with *Als,* or *Gar,* or *Sta,* or *Bio,* or *Chl*). This formidable number of possible reactions is thankfully reduced in natural assemblages due to meta- or instability of particular minerals in specific bulk compositions over the $P–T–H_2O$ ranges of metamorphism.

In balancing continuous reactions between AFM phases as many as five alternatives can be obtained (each above phase excluded in turn). The mineral formulae, shown in table 1, were used to obtain the stoichiometric coefficients for end-member reactions (see table 2) by means of the program REACTION (Finger and Burt, 1972; modified by D. Veblen,

[1] See Korzhinskii, 1959, p. 127.

TABLE 1

Simplified mineral formulae and activity models

Mineral name	Abbreviation	Simple formula	Activity model
Kyanite		Al_2SiO_5	
Andalusite		Al_2SiO_5	
Sillimanite	Als	Al_2SiO_5	
Kaolinite	Kas	$Al_2Si_2O_5(OH)_4$	
Pyrophyllite	Pyp	$Al_2Si_4O_{10}(OH)_2$	
Staurolite	Sta	$(Fe,Mg)_2Al_{26/3}Si_4O_{22}(OH)_2$	$(X_{Fe}^X)^2(X_{Al}^Y)^{8.667}$
Chloritoid	Ctd	$(Fe,Mg)Al_2SiO_5(OH)_2$	$(X_{Fe}^X)(X_{Al}^Y)^2$
Cordierite	Crd	$(Fe,Mg)_2Al_3(Al,Si_5)O_{18}$	$(X_{Fe}^X)^2(X_{Al}^Y)^3$
Garnet	Gar	$(Fe,Mg)_3Al_2Si_3O_{12}$	$(X_{Fe}^X)^3(X_{Al}^Y)^2$
*Chlorite	Chl	$[(Fe,Mg)_7Al_2][Al_2Si_4]O_{15}(OH)_{12}$	$(X_{Fe}^Y)^{7.5}(X_{Al}^Y)^{1.5}$
*Biotite	Bio	$K_3[(Fe,Mg)_6Al][Al_3(Al,Si_5)]O_{30}(OH)_6$	$(X_K^X)^3(X_{Fe})^9$
Muscovite	Mus	$KAl_3Si_3O_{10}(OH)_2$	
K-feldspar	Ksp	$KAlSi_3O_8$	
Quartz	Qtz	SiO_2	

* For substitutions of the type $Mg^OSi^T \rightleftharpoons Al^OAl^T$ (where O = octahedral, T = tetrahedral), enough excess Al is added to Si to fill tetrahedral sites, remaining Al is assigned to octahedral sites with Fe^{3+} and Ti. Note that these formulae for chlorite and biotite are used in all equations to avoid fractional quantities.

Harvard Univ.). The staurolite formulae $Fe_2Al_{26/3}Si_4O_{22}(OH)_2$ corresponds to 4 kyanite layers with an interlayer of $Al_{2/3}Fe_2O_4H_2$ (see Smith, 1968; Griffen and Ribbe, 1973). The cordierite formulae is taken to be anhydrous (this requires the equation of state of H_2O in the cordierite structure to be the same as that of a bulk H_2O-phase; P. C. Hess, personal commun.). Both chlorite and biotite are assumed to have one-third of the tetrahedral sites filled with alumina (compare Albee, 1962) and are treated only as Fe–Mg binary solutions. As can be seen from AFM diagrams most phases coexist with an aluminous biotite, although the formulae in table 1 do not necessarily define the maximum amount of alumina that these phases may contain. For biotite, the maximum alumina content achieved by the substitution (Mg,Fe)Si $\rightleftharpoons$ 2Al will occur in silica poor assemblages with phases that define the hypothetical component $KAl_7O_{10}(OH)_2$. In quartz bearing assemblages, this component is defined by muscovite coexisting with Als and Qtz, because

$$\mu KAl_7O_{10}(OH)_2 = \mu KAl_3Si_3O_{10}(OH)_2 + 2\mu Al_2SiO_5 - 5\mu SiO_2.$$

Other substitutions, such as those involving Fe^{3+} for Al or $2Al^{3+}$ + vacancy for $3(Fe^{2+},Mg^{2+})$, will require different assemblages to buffer the maximum alumina component.

For some bulk compositions low in alumina, continuous reactions may involve two-AFM phases of different alumina content (for example, *Gar–Bio*) with quartz, muscovite, *and* K-feldspar. On an AKFM projection from KAl_3O_5, SiO_2, and H_2O this would be represented by *Gar–Bio–Ksp*, and the biotite would contain less alumina than the cases discussed above and used in balancing the equations in table 2. For six-AFM phases (excluding Als) there are $6!/(4! \times 2!) = 15$ reactions between pairs of AFM phases with *Qtz, Mus,* and *Ksp*. Only a few of these will actually be observed, since they require a two-phase coexistence with *Ksp* in projection from KAl_3O_5, SiO_2, and H_2O.

Although different mineral formulae were used, the balanced equations in table 2 may be compared with those presented by J. B. Thompson (1972, p. 32, table 2).

Because a continuous reaction is a combination of two end-member reactions, the stoichiometric coefficients will be the same. Alternatively, the continuous reaction may be thought of as a combination of either end-member reaction with an Fe–Mg exchange reaction (see below). If Fe–Mg crystalline solutions of the phases *Crd, Chl, Bio, Ctd, Sta,* and *Gar* are ideal (with entropy of mixing arising only from random distribution), then the Fe–Mg partition between phases in two- and three-phase associations will be the same whatever the (Fe/Mg) bulk composition. This means that the Fe–Mg distribution coefficient (K_D) is a function of pressure and temperature only.

Discontinuous reactions.—In contrast to continuous reactions, discontinuous reactions reflect a distinct change in the topology of the AFM diagram. Because they generally affect a large range of bulk compositions and are independent of the proportions of relevant phases, discontinuous

reactions will in general produce easily observed changes in pelitic rocks and will therefore be the most suitable as isograds (J. B. Thompson, 1957, p. 856). The stoichiometric coefficients for a discontinuous reaction are not uniquely determined, except for specific P, T, and aH_2O. General solutions for these stoichiometric coefficients may be obtained using matrix methods (Korzhinskii, 1959, p. 91; Greenwood, 1967, 1975).

The general form of discontinuous reactions may be deduced from the relative positions of mineral compositions on the AFM projection and appropriate changes in topology. The $7!/(4! \times 3!)$ (= 35) possible discontinuous reactions are divided into *terminal* (disappearance or appearance of a phase within the AFM compositional field) and *non-terminal* (a given tie-line becomes metastable relative to a more stable tie-line) types in table 3. These terms are synonomous with *terminal invariant* and *diagonal invariant* of Ricci (1951, p. 218). The fact that X_{Mg} (*Sta-Ctd*) and X_{Mg} (*Chl–Bio*) are so close (almost colinear to Al_2O_3) means that under some circumstances the terminal or non-terminal nature of discontinuous reactions can only be proven by analysis of coexisting phases in the appropriate assemblages.

Fe–Mg–Mn distribution between coexisting AFM phases

Determination of the compositions of coexisting AFM phases indicate that the ratio Mg/Mg+Fe (called X_{Mg}) decreases in the order *Crd*> *Chl*>*Bio*>*Ctd*>*Sta*>*Gar* (see Albee, 1965a, b, 1972; Hess, 1969; Hensen, 1971). This distribution appears to be extremely regular, even for phases with comparable X_{Mg} (that is, almost colinear with A in the AFM projection; see Albee, 1965a, p. 513). The studies of Rumble (1971) and Albee (1972) indicate that $X_{Mg}^{Ctd} > X_{Mg}^{Sta}$. The work of Tewhey and Hess (1974) and Guidotti, Cheney, and Conatore (1975) suggest that the *Crd–Bio* join in the AFM projection passes on the Mg sides of the chlorite composition and that $X_{Mg}^{Crd} > X_{Mg}^{Chl} > X_{Mg}^{Bio}$, in contrast to the suggestion of Albee (1972, p. 3264 and figs. 13 and 14). The determination of X_{Mg} in these phases is difficult due to uncertain amounts of ferric iron.

The effect of Mn^{2+} on the Fe–Mg behavior may be predicted in similar fashion. Data from Osberg (1971, p. 583), Albee (1972, p. 3259), Tewhey and Hess (1974), and Guidotti (1974, fig. 7a) indicate that the ratio Mn/(Mn+Fe+Mg) decreases in the order *Gar*>*Ilm*(ilmenite)>*Ctd* >*Sta*>*Crd*>*Chl*>*Bio*.

In some cases complete AFM topologies have been constructed from the determination of the composition of coexisting phases for a wide range of AFM bulk rock compositions at the same grade (Albee, 1965a, p. 270; Guidotti, Cheney, and Conatore, 1975). The construction of specific "facies types", although unique only for given values of P, T, and aH_2O, provides important constraints on the behavior of specific continuous and discontinuous reactions in particular "facies series" (Thompson and Thompson, in preparation).

From a knowledge of the Fe/Mg partitioning between the near-ideal crystalline solutions, it is possible to predict the displacement of three-

TABLE 2

Continuous Mg–Fe and Fe–Mn reactions in pelitic rocks

(A) Continuous reactions involving 3-AFM phases (one of which is Als)

Since one phase is (Als) there are $6!/(4!\times 2!) = 15$ such reactions balanced with Mus *and/or* Ksp, Qtz, and H_2O. The degeneracy (Ctd–Crd, due to equal alumina content, or $(FeO+MgO)/Al_2O_3$ ratio) reduces this to 14.

	Als	Sta	Ctd	Crd	Gar	Chl	Bio	Mus	Ksp	Qtz	H_2O	T_{Mg}:T_{Fe}	T_{Fe}:T_{Mn}
(1) Als–Chl–Bio	−30					8	−7	21		−9	−48	>	<
(2) Als–Gar–Bio	5				−8		3		−9	22	−9	>	>
	−14				8		−3	9		−13		<(?)	<(?)
(3) Als–Crd–Bio	7			−4			1		−3	14	−3	<	>
	−10			4			−1	3		−11		>(?)	<(?)
(4) Als–Ctd–Bio	−10		8				−1	3		1	−8	>	<
(5) Als–Sta–Bio	−58	12					−3	9		7	−12	<	<
(6) Als–Gar–Chl	1				−7	3				8	−18	>	>
(7) Als–Crd–Chl	10			−7		2				17	−12	<	>
(8) Als–Ctd–Chl	−5		7			−1				2	−1	<	<
(9) Als–Sta–Chl	79	−21				6				−19	−15	>	>
(10) Als–Crd–Gar	−4			3	−2					−5		>	>
(11) Als–Ctd–Gar	−2		3		−1					2	−3	>	>
(12) Als–Sta–Gar	−11	3			−2					5	−3	>	>
(13) Als–Sta–Crd	−7	3		−3						10	−3	<	<
(14) Als–Sta–Ctd	7	−3	6							−1	−3	>	<

(B) Continuous reactions involving 3-AFM phases (none of which is Als)

Between 7-AFM phases there are a total of $7!/(3!\times4!) = 35$ reactions involving 3-AFM phases, 15 of which (with Als) are considered in (A) above. The remaining 20 are balanced with Mus *and/or* Ksp, Qtz, and H_2O. The degeneracy (Ctd-Crd) reduces this to 16.

	Als	Sta	Ctd	Crd	Gar	Chl	Bio	Mus	Ksp	Qtz	H_2O	T_{Mg}:T_{Fe}	T_{Fe}:T_{Mn}
(15) Gar–Chl–Bio					−30	14	−1	3		33	−84	>	>
(16) Crd–Chl–Bio				−3		2	−1	3		6	−12	<	<
(17) Crd–Gar–Bio				5	−14		4		−12	21	−12	>	>
				7	−10		2	−6		−3		>(?)	>(?)
(18) Crd–Gar–Chl				1	−10	4				9	−24	>	>
(19) Ctd–Chl–Bio			−6			2	−1	3		−3	−6	>	>
(20) Ctd–Gar–Bio			7		−5		1	−3		9	−7	>	>
(21) Ctd–Gar–Chl			1		−5	2				6	−13	>	>
(22) Sta–Chl–Bio		−90				116	−79	237		−183	−606	>	>
(23) Sta–Gar–Bio		42			−116		33	−99		213	−42	>	>
(24) Sta–Crd–Bio		30		−58			7	−21		177	−30	<	<
(25) Sta–Ctd–Bio		−30	116				−7	21		−3	−86	<	<
(26) Sta–Gar–Chl		3			−79	33				93	−201	>	>
(27) Sta–Crd–Chl		30		−79		14				219	−114	>	<
(28) Sta–Ctd–Chl		−15	79			−7				9	−22	<	<
(29) Sta–Crd–Gar		12		−33	14					75	−12	<	<
(30) Sta–Ctd–Gar		−6	33		−7					12	−27	>	>

The formulae used are presented in table 1. Note especially the biotite formula $K_3[(Fe,Mg)_6Al][Al_2(Al,Si_6)]O_{30}(OH)_6$ and the chlorite formula $[(Fe,Mg)_7Al_2][Al_2Si_4]O_{15}(OH)_{12}$. The reactions are written with the high entropy side (H_2O) as negative. The relative Mg–Fe end-member temperatures ($T_{Mg}>T_{Fe}$ or $T_{Mg}<T_{Fe}$) were deduced for $X_{Mg}^{Crd}>X_{Mg}^{Chl}>X_{Mg}^{Bio}>X_{Mg}^{Ctd}>X_{Mg}^{Sta}>X_{Mg}^{Gar}$ (where X_{Mg} = 100 Mg/Mg+Fe, see text). The relative Fe–Mn end-member temperatures were deduced for $X_{Mn}^{Gar}>X_{Mn}^{Ctd}>X_{Mn}^{Sta}>X_{Mn}^{Crd}>X_{Mn}^{Chl}>X_{Mn}^{Bio}$. In some cases more than one equation is presented for the case of (Mus) or (Ksp) absent. With the formulae used, there is a degeneracy between Ctd and Crd, since both have $(MgO+FeO)/Al_2O_3 = 1$. Thus the number of three-phase reactions will be reduced by 5, that is (Ctd–Crd) with Als, or Gar, or Sta, or Bio, or Chl will be replaced by (Ctd–Crd) in (A).

TABLE 3

Discontinuous Mg–Fe reactions in pelitic rocks

Between 7-AFM phases there are a total of $7!/(4!\times 3!) = 35$ reactions involving 4-AFM phases. By adding (Als) to the equations in Table 2(b) 20 discontinuous reactions are obtained, balancing with Mus *and/or* Ksp, Qtz and H_2O.

(A) Discontinuous reactions involving 4-AFM phases (one of which is Als)

Based upon X_{Mg} Crd>Chl>Bio>Ctd>Sta>Gar

Terminal to one-phase		Non-terminal (crossed tie lines)	
I	Ctd+Gar+Als–(Sta)	IX	Sta+Crd–(Ctd+Als)
II	Chl+Gar+Als–(Sta)	X	Sta+Chl–(Ctd+Als)
III	Crd+Gar+Als–(Sta)	XI	Sta+Bio–(Ctd+Als)
IV	Chl+Gar+Als–(Ctd)	XII	Sta+Crd–(Chl+Als)
V	Crd+Gar+Als–(Ctd)	XIII	Sta+Crd–(Bio+Als)
VI	Gar+Bio+Als–(Ctd)	XIV	Ctd+Crd–(Chl+Als)
VII	Bio+Gar+Als–(Sta)	XV	Ctd+Crd–(Bio+Als)
VIII	Bio+Crd+Als–(Chl)	XVI	Gar+Crd–(Chl+Als)
		XVII	Crd+Gar–(Bio+Als)
		XVIII	Sta+Chl–(Bio+Als)
		XIX	Ctd+Chl–(Bio+Als)
		XX	Gar+Chl–(Bio+Als)

(B) Discontinuous reactions involving 4-AFM phases (none of which is Als)

The remaining 35-20 = 15 reactions involving 4 AFM phases are:

Terminal to one-phase	Non-terminal (crossed tie lines)
XXI Sta+Crd+Gar–(Ctd)	XXVII Sta+Chl–(Ctd+Crd)
XXII Gar+Chl+Sta–(Ctd)	XXVIII Gar+Crd–(Ctd+Chl)
XXIII Bio+Ctd+Crd–(Chl)	XXIX Gar+Crd–(Chl+Sta)
XXIV Gar+Crd+Bio–(Chl)	XXX Gar+Crd–(Ctd+Bio)
XXV Gar+Bio+Sta–(Ctd)	XXXI Bio+Sta–(Ctd+Crd)
XXVI Bio+Sta+Crd–(Chl)	XXXII Gar+Chl–(Bio+Sta)
	XXXIII Gar+Chl–(Bio+Ctd)
	XXXIV Gar+Crd–(Bio+Sta)
	XXXV Bio+Sta–(Ctd+Chl)

phase AFM fields as functions of varying pressure, temperature, and aH_2O.

PREDICTION OF CHANGES IN THE AFM PROJECTION

It has been noted by several workers that certain three-phase associations in the AFM diagram become *more Fe-rich with increasing grade.* Specific examples include *Bio–Crd–Als–Qtz–Ksp* (Best and Weiss, 1964; Hess, 1969) and *Bio–Sta–Als–Qtz–Mus* (Chinner, 1965; Hess, 1969; Guidotti, 1970, 1974). In some natural assemblages, for example *Chl–Crd–Bio–Qtz–Mus,* it is not clear whether the apparent Fe enrichment is the result of increasing grade or variation in aH_2O (see Tewhey and Hess, 1974; Guidotti, Cheney, and Conatore, 1975).

By means of the continuous reaction coefficients presented in table 2, it is possible to distinguish the hydration from the dehydration reactions. It is assumed, as is generally the case, that water is part of the high-entropy and hence high-temperature assemblage for reactions involving dehydration. Thus, from a knowledge of the relative Fe/Mg ratio of the phases involved in a continuous dehydration reaction, the displacement of any particular three-phase assemblage due to changing temperature or

aH_2O may be predicted. The relative temperatures for the Fe–Mg and Fe–Mn end-member reactions deduced in this way are shown in table 2 (columns T_{Mg}:T_{Fe} and T_{Fe}:T_{Mn}). Similarly, the displacement of a particular three-phase association with changing pressure (that is, P_{Mg}:P_{Fe} or P_{Fe}:P_{Mn}) may be predicted from Fe/Mg or Fe/Mn partitioning and $\Delta\bar{V}°$ for end-member reactions, at constant T and aH_2O. In addition these may be related to displacements in a P–T projection without knowledge of absolute $\Delta\bar{S}$, provided that H_2O forms part of the high-temperature assemblage. From the equilibrium approximations,

$$\Delta T = \frac{nRT\ln K}{\Delta\bar{S}°} \qquad \text{and} \qquad \Delta P = \frac{-nRT\ln K}{\Delta\bar{V}°}$$

it can be seen that for dehydration reactions with relatively large values of $\Delta\bar{S}°$ and $\Delta\bar{V}°$, small changes in T, P, or aH_2O would result in large changes in composition of coexisting phases. Conversely for anhydrous equilibria with much smaller values of $\Delta\bar{S}°$ and $\Delta\bar{V}°$, large changes in T or P would result in only small changes in composition of coexisting phases. For these latter equilibria, estimation of dP/dT from measured or estimated volume and entropy data can sometimes lead to the wrong high-entropy assemblage if configurational contributions to entropy are neglected.

CONTINUOUS REACTIONS AS T–X OR P–X LOOPS

The behavior of three-phase associations in the AFM diagram, representing continuous reactions, may be represented by *pseudo*-binary T–X(Fe–Mg) and P–X(Fe–Mg) diagrams (see Ramberg, 1944; Hensen, 1971; Albee, 1972). In addition to assuming saturation with *Mus* (or *Ksp*), *Qtz*, and H_2O (by virtue of the AFM projection), the sections are projected from Al_2O_3 onto an arbitrary Fe–Mg plane. They superimpose planes taken at specific values of A (for example, the garnet–chlorite and chloritoid–cordierite joins described by Albee, 1972, figs. 13 and 14). This construction can be better seen with the "parallel edge AFM projection" of J. B. Thompson (1957, figs. 7 and 8), where A corresponds to the molar quantity $(Al_2O_3–3K_2O)/(MgO+FeO)$. Although some three-phase assemblages do not contain Als, the *pseudo*-binary construction shows the relative X_{Mg} of phases defined only as binary Fe–Mg solutions.

Three-phase assemblages not containing *Als* actually define a lower μAl_2SiO_5 (or μAl_2O_3, since quartz is assumed to be present) than assemblages where one of the three AFM phases is *Als*.

As an example, consider the continuous (Fe–Mg) reactions (the stoichiometric coefficients for which are presented in table 2).

$$\text{Chl} + \text{Mus (Sta)} \quad \text{Bio} + \text{Als} + \text{Qtz} + H_2O \qquad (1)$$

$$\text{Sta} + \text{Mus} + \text{Qtz (Chl)} \quad \text{Bio} + \text{Als} + H_2O \qquad (5)$$

$$\text{Chl} + \text{Als (Bio)} \quad \text{Sta} + \text{Qtz} + H_2O \qquad (9)$$

$$\text{Chl} + \text{Mus (Als)} \quad \text{Sta} + \text{Bio} + \text{Qtz} + H_2O \qquad (22)$$

where the phase in brackets is the absent phase, following the notation of Schreinemakers (1915-1925, see Zen, 1966). These continuous reactions intersect at the discontinuous (Fe–Mg) reaction (table 3, XVIII)

$$\text{Sta} + \text{Chl} + \text{Mus} = \text{Bio} + \text{Als} + \text{Qtz} + \text{H}_2\text{O} \qquad \text{(XVIII)}.$$

These reactions are shown as divariant loops in a schematic pseudobinary T–X(Fe–Mg) section in figure 1A and illustrate the discontinuous reaction described by Guidotti (1974, p. 487) for the case of sillimanite (*Als* = *Sil*). At the isobaric temperature of the discontinuous (Fe–Mg) reaction the compositions of the phases *Sta*, *Bio*, and *Chl* are uniquely defined.

Above and below the discontinuous reactions, the compositions of individual phases are represented by the appropriate (three-phase) continuous reactions. The isobaric continuous reactions terminate at the temperatures for the appropriate reactions in the end-member systems (KMASH and KFASH). Relative end-member temperatures may be determined from isobaric sections across P–T diagrams. The P–T diagrams for reactions in the pure Fe-system (KFASH) were constructed using methods similar to those used by Hoschek (1969, fig. 5). They are further constrained by the orientation of univariant curves around the P–T invariant points and the resultant geometry of T–X and P–X sections.

Superimposition of T–X loops and progressive metamorphism.—At temperatures below the isobaric discontinuous reaction (XVIII, Mus + Sta + Chl = Bio + Als) the phases *Sta* and *Chl* in the association *Sta–Chl–Bio* are more Fe-rich than those in the association *Sta–Chl–Als* (compare the AFM diagrams in fig. 1A and in Guidotti, Cheney, and Conatore, 1975). The discontinuous reaction (XVIII) is thus defined where the compositions of *Sta* and *Chl* in the *Sta–Chl–Bio* and *Sta–Chl–Als* associations become identical, and the two-phase field *Sta–Chl* is eliminated. At temperatures above the isobaric discontinuous reaction (XVIII), the association *Sta–Bio–Als* becomes more Fe-rich, whereas the association *Chl–Bio–Als* becomes more Mg-rich, for the coefficients in table 2 and predicted values of T_{Mg}:T_{Fe}. Albee (1972, p. 3264) discusses the possibility that divariant loops on a T–X(Fe–Mg) diagram may "tail down" if the Fe end-member reaction occurs at a higher temperature than the Mg end-member reaction ($T_{Fe}>T_{Mg}$). He considers this to be unlikely and suggests that the continuous reaction (*Bio–Sta–Als–Qtz–Mus*) becomes more Mg-rich with increasing grade (Albee, 1972, figs. 13 and 14).

Discontinuous reactions are thus completely defined when the compositions of individual phases in the three-phase associations coincide. These compositions will change for different temperatures and pressures along the "univariant" discontinuous reaction. Other continuous reactions not involved in the particular discontinuous reaction (for example, *Chl–Crd–Als*) are indifferent to the reaction and merely continue through on T–X sections (see fig. 2). Although not shown in fig. 1, the relative Fe–Mg location of the indifferent continuous reactions may be obtained from the AFM diagram for the facies type.

Schematic T–X(Fe–Mg) sections constructed on the principles outlined above are presented in figure 1 (A to D) for the discontinuous reactions

$$\text{Gar} + \text{Chl} + \text{Mus} = \text{Sta} + \text{Bio} \quad \text{(non-terminal type)} \quad \text{(XXXII)}$$

$$\text{Sta} + \text{Chl} + \text{Mus} = \text{Bio} + \text{Als} \quad \text{(non-terminal type)} \quad \text{(XVIII)}$$

$$\text{Chl} + \text{Mus} = \text{Bio} + \text{Crd} + \text{Als} \quad \text{(terminal type)} \quad \text{(VIII)}$$

$$\text{Sta} + \text{Mus} = \text{Bio} + \text{Gar} + \text{Als} \quad \text{(terminal type)} \quad \text{(VII)}.$$

These individual discontinuous reactions have been combined on a composite isobaric T–X(Fe–Mg) section in figure 2. This schematic sequence represents part of a progressive Barrovian type facies series, for PH_2O of about 5 to 6 kb (compare fig. 5 in pt. II and Hess, 1969, fig. 3; 1973). Depending upon the choice of P–T locations of the Al_2SiO_5 phase relations, the three-phase associations *Sta–Bio–Als*, *Bio–Chl–Als*, *Chl–Crd–Als*, and *Bio–Crd–Als* would undergo inflections at the appropriate Al_2SiO_5 univariant curves. If the dP/dT slopes of end-member reactions change sign across the Al_2SiO_5 transition, it is possible that this could reverse the trend of Fe/Mg enrichment for a particular continuous reaction. To avoid further complication the *Kya–And*, *Kya–Sil*, or *And–Sil* transitions have been omitted from figure 2, but field evidence suggests that in a Barrovian metamorphic sequence the *Kya–Sil* transition occurs at conditions above the discontinuous reaction (XVIII, Sta + Chl + Mus = Bio + Als). Reactions involving chloritoid (*Ctd*) have not been included in figure 2, nor have the reactions leading to the facies type shown on the AFM diagram at the lower right.

Reversals in P–X and T–X loops due to extremal states.—Reversals in Fe–Mg distribution are unlikely because of the near ideality of the substitution (see J. B. Thompson, 1957, p. 857). Only non-ideality (possibly due to significant Fe–Mg ordering in distinct crystallographic sites) could result in the reversal of X_{Mg} between a pair of coexisting Fe–Mg phases. Thus an *extremal state* (where the reversal in X_{Mg} corresponds to a maximum or minimum on a (pseudo-) binary T–X(Fe–Mg) or P–X(Fe–Mg) transition loop (Korzhinskii, 1963) is not possible for coexisting ideal solutions that have different X_{Mg} across the whole composition range (as noted by Albee, 1972, p. 3263). It is not known whether some observed compositional colinearities, near to the Fe or Mg end-member limits (for example, *Gar–Sta*, *Sta–Ctd*, *Bio–Chl*), represent non-ideality of crystalline solution or reflect difficulties in chemical analysis.

Divariant reactions involving biotite.—Only reactions in the K–muscovite plus quartz field have been considered in figure 2. Some reaction loops, specifically those involving biotite, may change the direction of Fe/Mg enrichment with increasing temperature at the reaction

$$KAl_3Si_3O_{10}(OH)_2 + SiO_2 = KAlSi_3O_8 + Al_2SiO_5 + H_2O.$$

Consider the reactions involving *Bio–Crd–Gar–Als–Qtz* with either *Mus* or *Ksp*. A schematic pseudobinary T–X(Fe–Mg) section for the continuous

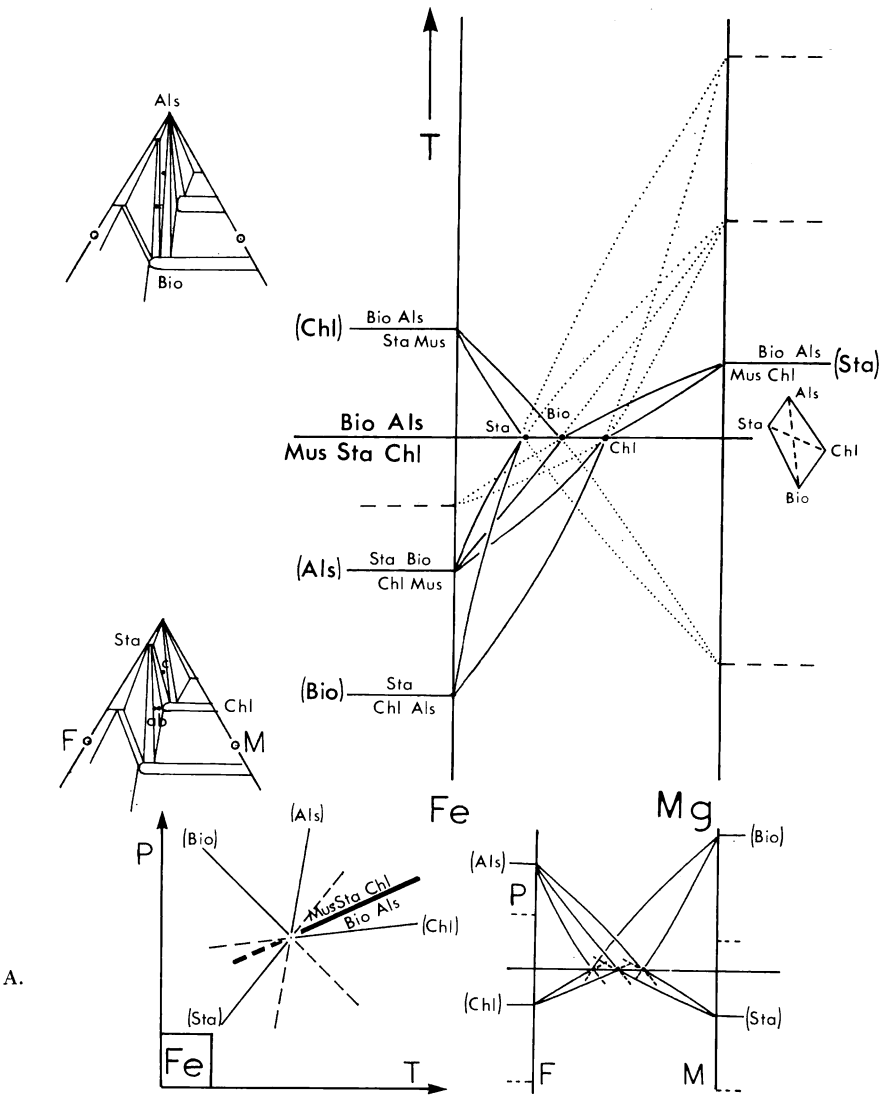

A.

Fig. 1. Schematic AFM diagrams (projected from KAl_5O_5, SiO_2, H_2O), P–T diagrams for end-member reactions in KFASH and isobaric T–X(Fe–Mg) sections for continuous and discontinuous reactions discussed in the text and tables 1, 2, and 3. (A) reaction XVIII [*Mus* + *Sta* + *Chl* = *Bio* + *Als*]; (B) reaction XXXII [*Mus* + *Gar* + *Chl* = *Sta* + *Bio*]; (C) reaction VIII [*Mus* + *Chl* = *Bio* + *Crd* + *Als*]; (D) reaction VII [*Sta* +*Mus* = *Gar* + *Bio* + *Als*]. The skeleton diagrams at the discontinuous reactions show the *non-terminal* or *terminal* nature of the transitions. The P–T diagrams are oriented from natural diagrams and estimated entropy data (see pt. II). Schematic isothermal P–X(Fe–Mg) diagrams, predicted from volume data, are shown as insets.

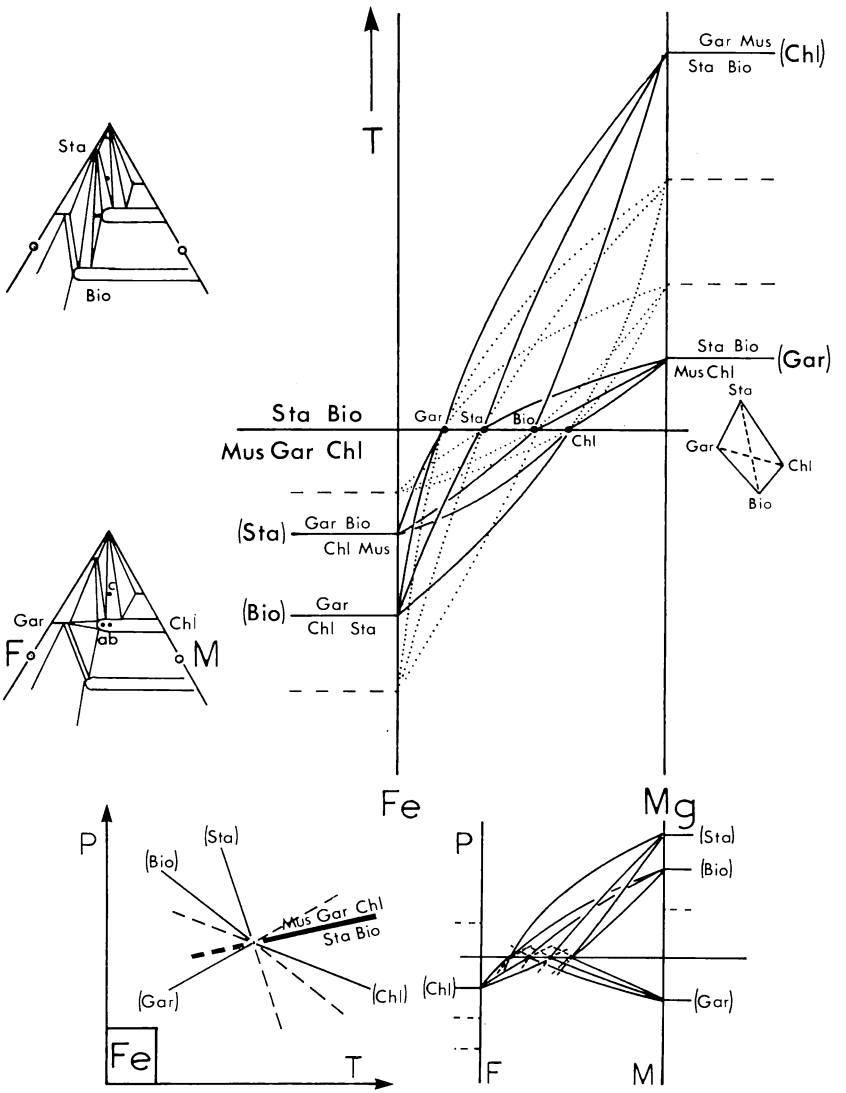
Sta
Bio
T
Gar Mus
Sta Bio
(Chl)
Sta Bio
(Gar)
Mus Chl
Sta
Gar
Chl
Bio
Sta Bio
Mus Gar Chl
Gar
Sta
Bio
Chl
(Sta)
Gar Bio
Chl Mus
(Bio)
Gar
Chl Sta
Gar
Chl
F
M
ab
Fe
Mg
P
(Sta)
(Bio)
Mus Gar Chl
Sta Bio
(Gar)
(Chl)
Fe
T
P
(Sta)
(Bio)
(Chl)
(Gar)
F
M

Fig. 1B.

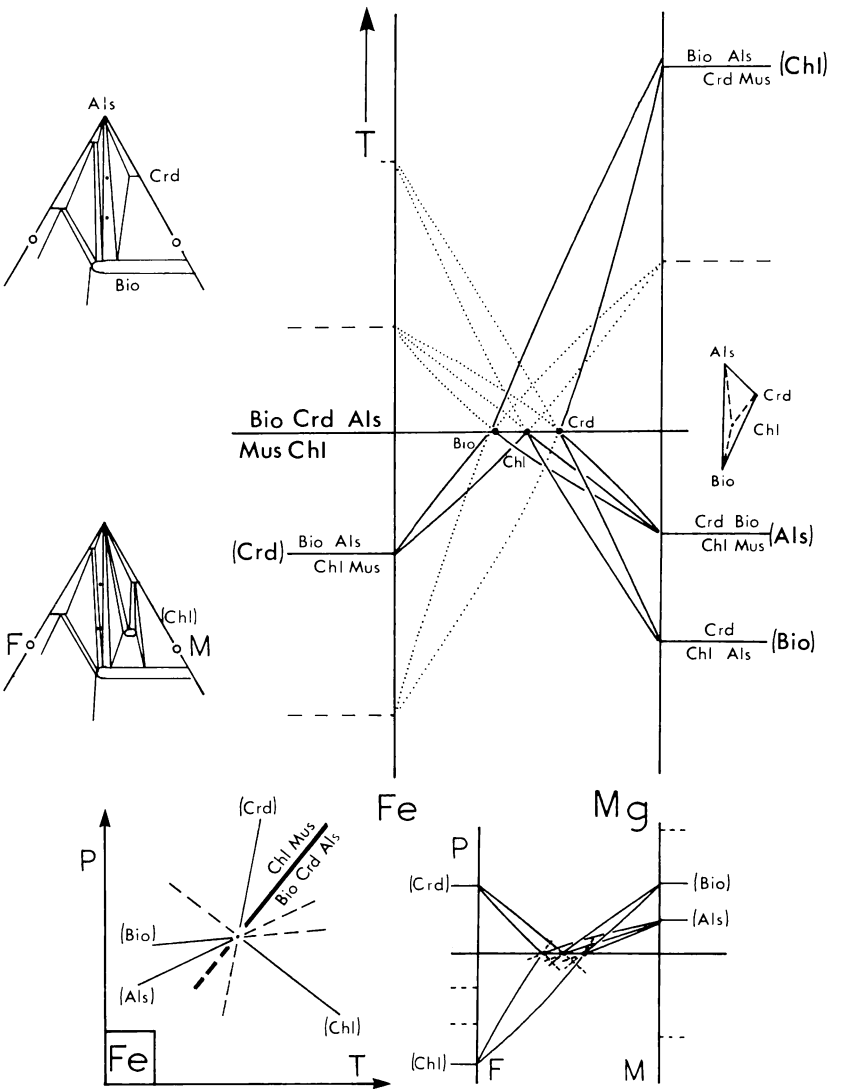
Als
Crd
Bio
(Chl)
F
M
T
Bio Als / Crd Mus (Chl)
Bio Crd Als / Mus Chl
Bio
Chl
Crd
(Crd) Bio Als / Chl Mus
Crd Bio / Chl Mus (Als)
Crd / Chl Als (Bio)
Als
Crd
Chl
Bio
Fe
Mg
P
(Crd)
Chl Mus
Bio Crd Als
(Bio)
(Als)
(Chl)
Fe
T
P
(Crd)
(Bio)
(Als)
(Chl)
F
M

Fig. 1C.

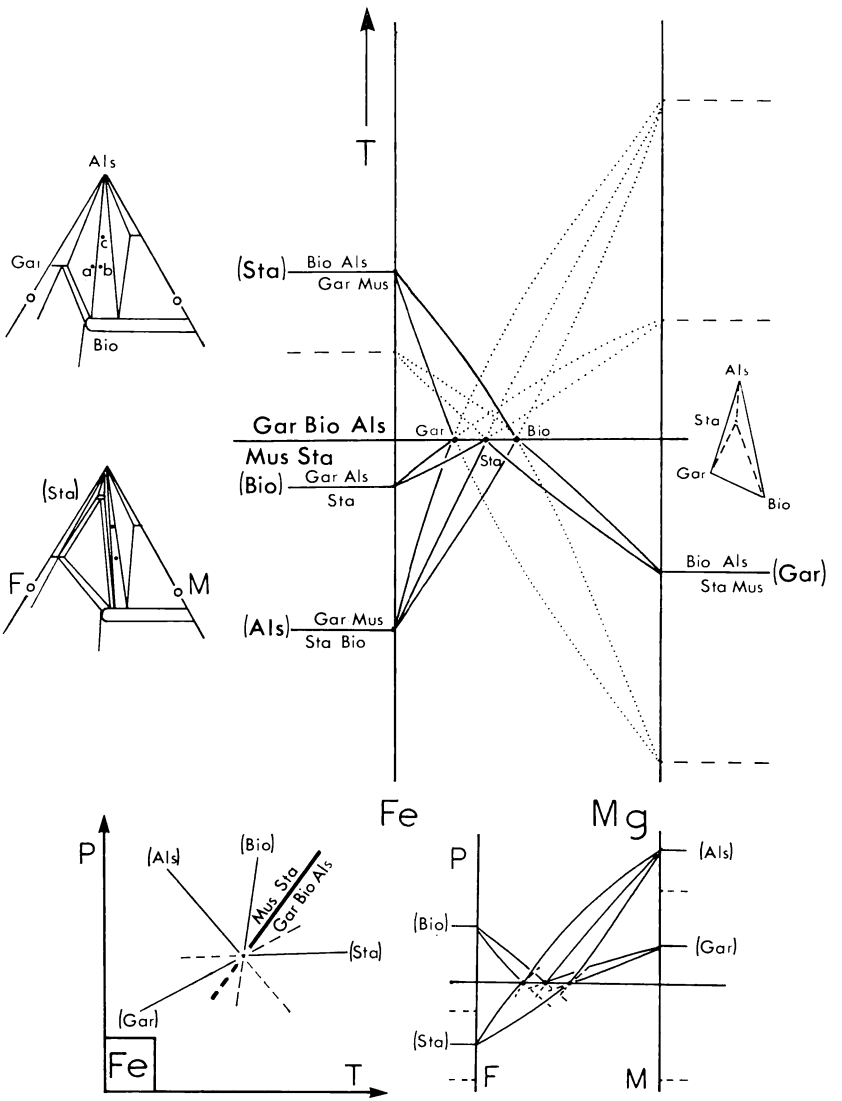
Als
Gar
c
a
b
Bio
(Sta)
Fo
M
T
(Sta) Bio Als / Gar Mus
Gar Bio Als
Mus Sta
(Bio) Gar Als / Sta
(Als) Gar Mus / Sta Bio
Gar
Bio
Sta
Als
Sta
Gar
Bio
Bio Als / Sta Mus (Gar)
Fe
Mg
P
(Als)
(Bio)
Mus Sta
Gar Bio Als
(Sta)
(Gar)
Fe
T
P
(Als)
(Bio)
(Gar)
(Sta)
F
M

Fig. 1D.

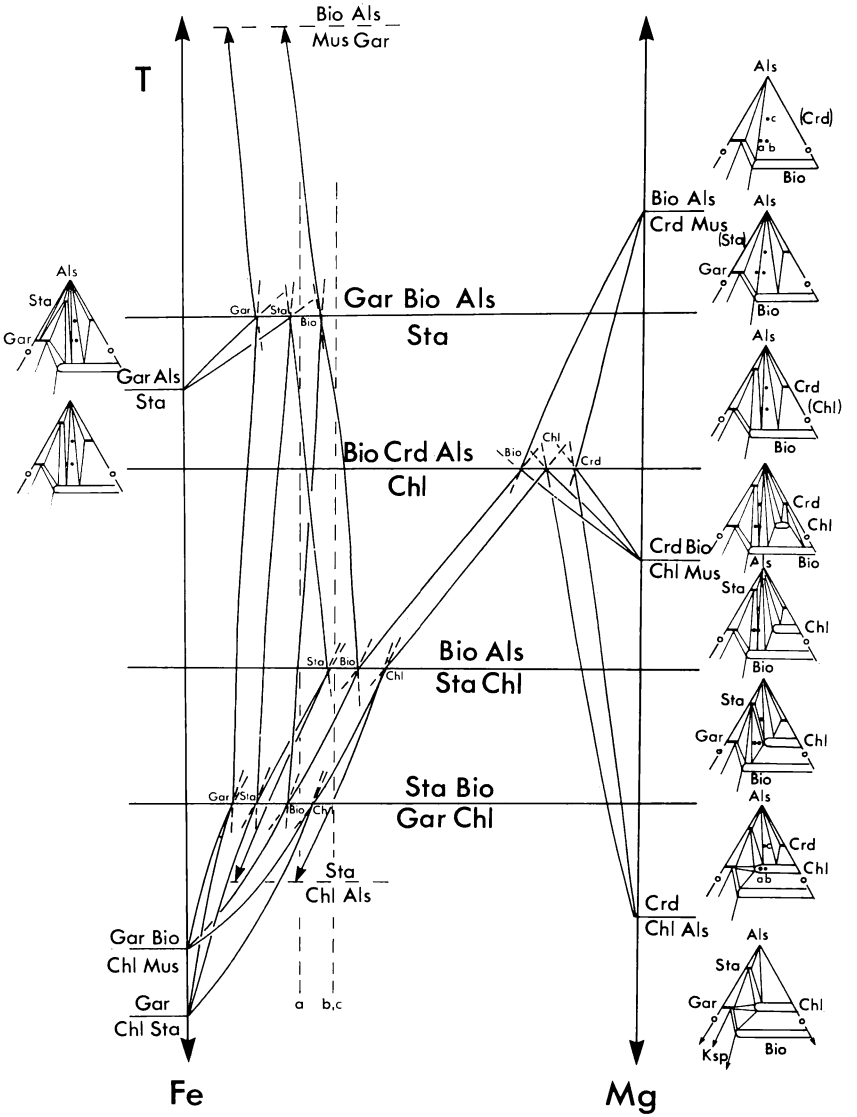

Fig. 2. Composite T–X(Fe–Mg) diagram for the sequential continuous and discontinuous reactions (XXXII, XVIII, VIII, VII) in figure 1, involved in a Barrovian-type facies series ($PH_2O \approx 5$ kb) below the disappearance of *Mus* + *Qtz*. The mineral assemblages observed for progressive metamorphism of compositions *a*, *b*, and *c* are discussed in the text (see also fig. 1). The location of end-member temperatures (T_{Fe}:T_{Mg}) for continuous reactions that are "indifferent" to the various discontinuous reactions are schematic. Note that the three-phase regions *Chl–Crd–Bio* and *Sta–Gar–Als* appear just below the discontinuous reactions *Mus* + *Chl* → *Bio* + *Crd* + *Als* and *Sta* + *Mus* → *Gar* + *Bio* + *Als*, respectively.

reactions in the *Mus–Qtz* field is shown in figure 3A. The continuous reactions (the stoichiometric coefficients are presented in table 2)

$$\text{Mus} + \text{Gar} \rightarrow \text{Bio} + \text{Als} + \text{Qtz} \quad (2)$$

$$\text{Mus} + \text{Crd} \rightarrow \text{Bio} + \text{Als} + \text{Qtz} \quad (3)$$

$$\text{Crd} \rightarrow \text{Gar} + \text{Als} + \text{Qtz} \quad (10)$$

$$\text{Bio} + \text{Crd} \rightarrow \text{Gar} + \text{Mus} + \text{Qtz} \quad (17)$$

are all (H_2O)-absent reactions, at least for the case of anhydrous cordierite as used here. However, Schreyer and Siefert (1969) suggest that for the Mg end-member reaction (3), *Bio + Als* form the high temperature assemblage. Richardson (1968) and Weisbrod (1973) suggest that for the Fe end-member reaction (10), *Gar + Als + Qtz* form the high-temperature assemblage. If the cordierite in the experimental charges contained structural water, then some of the above reactions would involve dehydration.

At temperatures above the reaction of K–muscovite plus quartz to K–feldspar plus Al_2SiO_5, the high temperature side of the continuous reactions involving *Bio–Crd–Gar–Ksp–Qtz* may be determined (table 2), since reactions (2), (3), and (17) involve dehydration. A schematic T–X(Fe–Mg) section for these reactions is presented in figure 3B. A comparison of figures 3A and B suggests that $T_{Fe}>T_{Mg}$ for the continuous reaction (2), that is, Mus + Gar → Bio + Als + Qtz, whereas $T_{Mg}>T_{Fe}$ for the continuous reaction Bio + Als → Gar + Ksp + H_2O. These relative end-member temperatures for the continuous reaction involving Ksp are supported by the observations of Best and Weiss (1964), Reinhardt (1968), and Dougan (1974) on natural assemblages. Similarly, the continuous reaction Crd + Mus → Bio + Als + Qtz has $T_{Mg}>T_{Fe}$ (see Seifert, 1970), whereas the reaction Bio + Als + Qtz → Crd + Ksp + H_2O has $T_{Fe}>T_{Mg}$ (see Best and Weiss, 1964; Reinhardt, 1968; and Dougan, 1974).

The discontinuous reaction (XVII, table 3) with *Mus–Qtz* has *Bio–Als* on the high temperature side such that *Gar–Bio–Crd* and *Gar–Crd–Als* are stable at lower temperatures and *Bio–Gar–Als* and *Bio–Crd–Als* are stable at higher temperatures. This situation is reversed with *Ksp–Qtz* assemblages (see fig. 3 in this paper and fig. 3B in pt. II), since the discontinuous reaction (XVII) has a negative dP/dT slope in the *Mus–Qtz* field and a positive slope in the *Ksp–Qtz* field. It should be emphasized that the values of dP/dT are strongly dependent upon the water content of cordierite and the resulting stoichiometric coefficients (see Hess, 1969, p. 196).

The fact that some continuous reactions have $T_{Fe}>T_{Mg}$ (where the minerals in three-phase associations become more Fe-rich with increasing temperature) and that this may reverse for biotite reactions involving *Ksp–Qtz* instead of *Mus–Qtz* has significant implications for studies concerned with the variation of composition of *individual* minerals with increasing metamorphic grade.

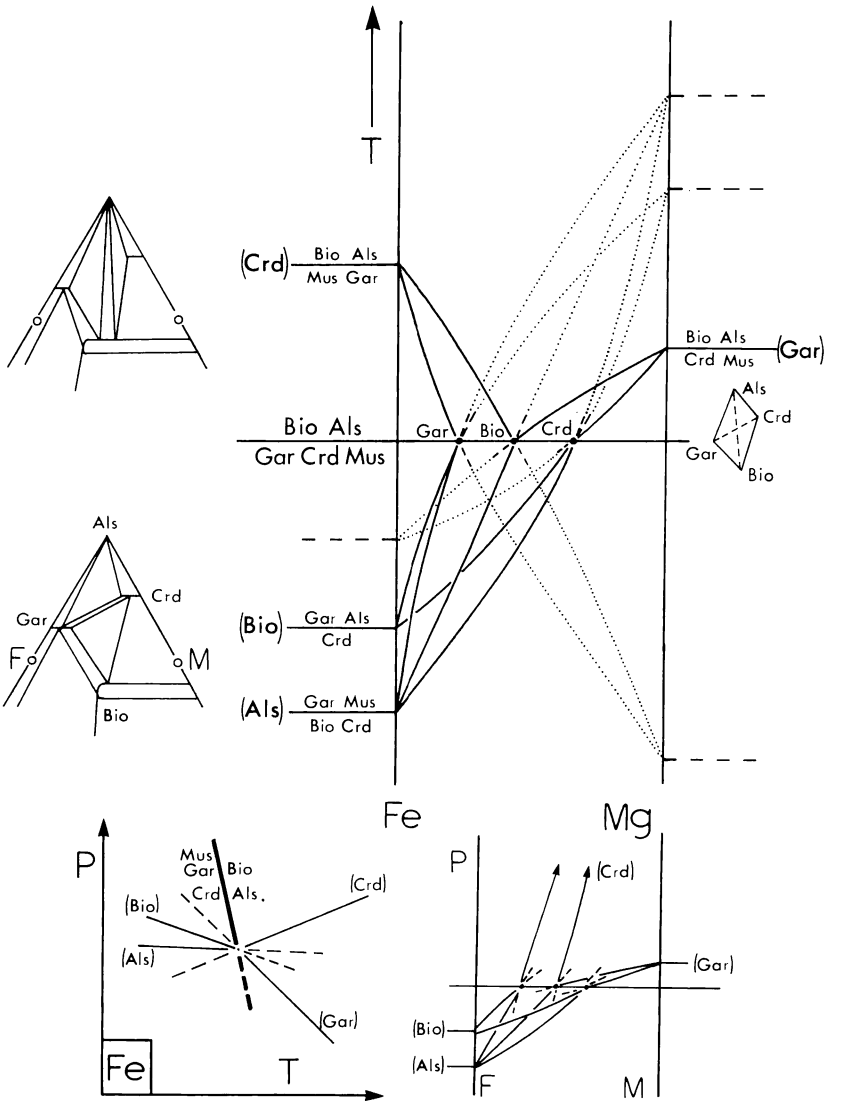

A.

Fig. 3. Schematic AFM diagrams (projected from SiO_2, H_2O, KAl_5O_5 *or* $KAlO_2$), P–T diagrams for KFASH, isobaric T–X(Fe–Mg) and isothermal P–X(Fe–Mg) sections for continuous and discontinuous reactions involving *Gar–Bio–Crd–Als–Qtz* (XVII) with (A) *Mus* and (B) *Ksp*. In (A) the discontinuous reaction (*Mus* + *Gar* + *Crd* = *Bio* + *Als*) has *Bio* + *Als* as the high-temperature assemblage, whereas in (B) the reaction (*Bio*+ *Als* = *Gar* + *Crd* + *Ksp*) has *Gar* + *Crd* + *Ksp* as the high temperature assemblage. The continuous reactions involving *Bio–Gar–Als* and *Bio–Crd–Als* undergo inflections at the reaction (*Mus* + *Qtz* = *Ksp* + *Als* + H_2O). The discontinuous reaction involving *Mus* may have a very limited stability in P–T space. The relations in (B) involve *Ksp, Qtz, and* H_2O, and thus *Gar* may coexist with pure Fe-biotite unless a phase with greater X_{Fe} and lower-alumina content than biotite is present.

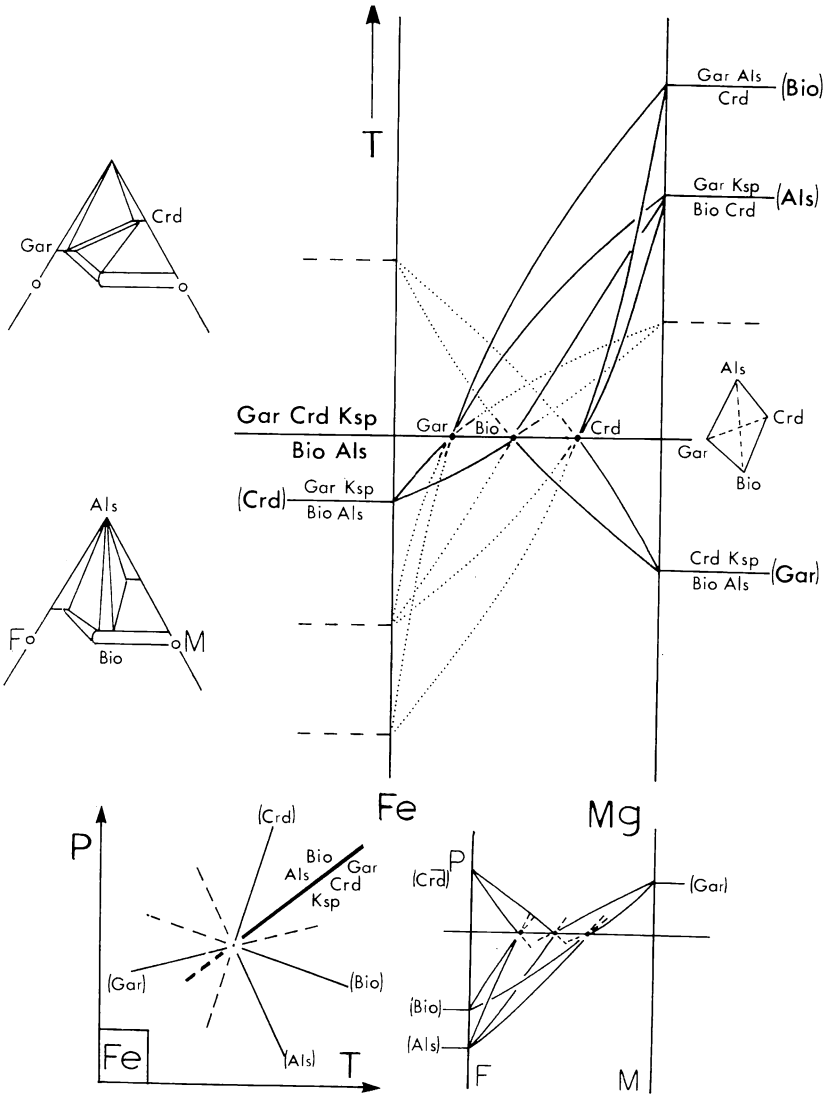
Gar
Crd
Als
Fo
M
Bio
T
Gar Als / Crd (Bio)
Gar Ksp / Bio Crd (Als)
Gar Crd Ksp
Bio Als
Gar
Bio
Crd
(Crd) Gar Ksp / Bio Als
Crd Ksp / Bio Als (Gar)
Fe
Mg
P
(Crd)
Bio
Als
Gar
Crd
Ksp
(Gar)
(Bio)
(Als)
T
F
M

Fig. 3B.

VARIATION OF MINERAL COMPOSITION WITH METAMORPHIC GRADE

Many studies have been concerned with the variation of the composition of *individual* minerals with metamorphic grade. In many cases the specific paragenesis has not been reported, and slight variations in composition have been ascribed to inaccuracy of analysis, which in some cases is no doubt justified. Some significant observations of compositional variation with increasing grade can be made by reference to the schematic T–X(Fe–Mg) sections in figures 1 and 2.

Continuous (Fe–Mg) reactions in T–X (or P–X) sections may be viewed in the same way as simple liquidus diagrams between ideal liquid and crystalline solutions. The continuous reaction loop may cross over the bulk composition moving from a three-phase to two-phase region in the same way that complete melting or complete crystallization is related to bulk composition on the liquidus–solidus diagram. For a two-phase region between two ferromagnesian phases, their Fe/Mg ratio is limited by the continuous reactions defining the adjacent three phase regions on the AFM diagram. For a bulk composition falling in a two-phase region between ferromagnesian phases, changing pressure or temperature (*but not* aH_2O, see pt. II) will result in Fe–Mg exchange between the phases giving the appearance of "tie-line rotation." In actual fact this will be difficult to observe because K_D(Fe–Mg distribution coefficient) will not vary much over the small temperature range that the bulk composition will be represented by a two-phase region. If a bulk composition lies exactly at the Al_2O_3/(FeO+MgO) ratio of a single AFM phase or lies in a two-phase field between a single AFM phase and Als, the AFM phase will have the Fe/Mg ratio of the bulk composition, unless an iron oxide or sulphide phase is present. For this case the compositional variation of an individual phase may bear no relation to grade.

Consider a pelitic rock sequence where different bulk compositions are found in adjacent beds. Compositions *a* and *b* (solid circles in the AFM diagrams in figs. 1 and 2) have an alumina content near *Chl* in the projection, but *a* is slightly richer in iron than *b*. Compositions *b* and *c* have the same Fe/Mg ratio, but *c* is richer in alumina. At temperatures below the discontinuous reaction (XXXII, Gar + Chl + Mus = Sta + Bio, figs. 1B and 2) compositions *a* and *b* would be represented by *Chl*, *c* would be represented by *Chl–Als*, whereas more Fe-rich compositions would have passed the "garnet isograd" (*Gar–Chl–Bio*) or even "garnet and staurolite isograds" (*Sta–Gar–Chl*). At temperatures above the discontinuous reaction (XXXII) compositions *a* and *b* are represented by *Sta–Bio–Chl*, and *c* is represented by *Sta–Chl–Als* (figs. 1B and 2). With increasing temperature both the assemblages *Sta–Bio–Chl* and *Sta–Chl–Als* (and hence the three-phase triangles) move toward more Mg-rich compositions until the discontinuous reaction (XVIII, Sta + Chl + Mus = Bio + Als) is reached (figs. 1A and 2). For both *a* and *b*, *Sta–Bio* increase at the expense of *Chl*. For *a*, *Chl* will be eliminated before (XVIII) is reached, and only *Sta–Bio* will be observed (figs. 1A and 2). At temperatures above (XVIII), compositions *b* and *c* will be represented by *Sta–*

Bio–Als with greater amounts of *Bio* in *b* and *Sta–Als* in *c* (figs. 1A and 2). Not only will *Sta* be consumed at the expense of *Bio–Als* with increasing temperature, but both phases will become more iron-rich. Although *a* will be represented by *Sta–Bio* above (XVIII), further increase in temperature will result in composition *a* producing *Bio–Als* at the expense of *Sta* as the three-phase triangle *Sta–Bio–Als* "sweeps across" composition *a* (figs. 1A and 2). By the same token, *Sta* will disappear from compositions *b* and *c* (now represented by the two-phase field, *Bio–Als*) *before* discontinuous reaction (VII, Sta + Mus → Bio + Gar + Als) is reached (figs. 1D and 2). At temperatures above discontinuous reaction (VII) compositions *b* and *c* will be represented by *Bio-Als*, whereas *a* will be represented by *Gar–Bio–Als* (figs. 1D and 2). Thus the "garnet isograd" for *a* will lie at higher temperatures than for bulk compositions initially richer in iron. With increasing temperature for composition *a*, both *Gar* and *Bio* become more iron-rich along with increased modal amounts of biotite at the expense of garnet until only *Bio–Als* remain (figs. 1D and 2). The biotite composition in the two-phase association *Bio–Als* is no longer constrained in Fe/Mg ratio, and if this is the only ferromagnesian mineral in the rock, it will have the same Fe/Mg ratio as the bulk composition (in the absence of iron oxides and sulphides).

Although the above examples are purely schematic they serve to show that for a particular bulk composition an *individual mineral* (for example, biotite) may reverse its trend of Fe/Mg enrichment with increasing grade, depending upon the associated AFM phases and the continuous reactions relating them. These slight compositional variations are frequently averaged and significant details of the progressive metamorphic history are lost.

DISCONTINUOUS REACTIONS IN NATURAL ASSEMBLAGES

Although discontinuous reactions in KFMASH will in general be observed easily in a wide range of pelitic rock compositions, they are rarely abrupt in metamorphic sequences. The participation of other components in the reactions often results in the KFMASH discontinuous reactions being continuous in a more complex chemical system. The effect of Na on mica–feldspar equilibria was referred to above. Similarly, the presence of Mn often results in ternary (Fe–Mg–Mn) continuous reactions frequently stabilizing assemblages (particularly garnet-bearing) outside their (Fe–Mg) stability ranges, as does Ca through garnet–plagioclase continuous reactions (Tracy, Robinson, and Thompson, in press). Not only do phase relations in KFMASH provide a useful model for metamorphism of pelitic rocks, but continuous reactions involving additional components may simply be related to KFMASH equilibria through exchange reactions (see pt. II).

In part II, compositional data on AFM assemblages have been combined with available experimental and thermochemical data in an attempt to provide pressure and temperature calibration of some continuous and discontinuous reactions.

In both parts I and II the continuous and discontinuous (Fe–Mg) reactions are considered only for the case of a fixed value of Al_2O_3/(FeO+MgO). In view of the fact that the model system KFMASH does not contain Na_2O and CaO, phase relations will not be affected by such alumina-producing reactions as

$$NaAl_2(AlSi_3)O_{10}(OH)_2 = NaAlSi_3O_8 + (Al_2O_3) + H_2O$$

which occur in natural assemblages concurrently with those in KFMASH. As discussed by J. B. Thompson and Norton (1968, p. 322, eq 1 and 4) a combination of the above reaction, which effectively releases (Al_2O_3), with a reaction in KFMASH will displace projected bulk compositions in AKFM toward (Al_2O_3). Similar effects could be produced through simultaneous reaction of the calcium phases, epidote, margarite, and plagioclase, where the bulk compositions would be displaced toward or away from (Al_2O_3) as appropriate. Reactions between iron oxides, iron-titanium oxides, iron sulphides, graphite, or siderite and Fe–Mg silicates will displace projected bulk compositions away from or toward (FeO) as appropriate (J. B. Thompson, 1972, p. 31).

An additional substitution in KFMASH, not specifically considered here, is the Tschermak's substitution of muscovite toward phengite (involving $Al_2(Fe,Mg)_{-1}Si_{-1}$). Reactions involving changing phengite content of muscovite can also displace projected bulk compositions in AKFM toward or away from (Al_2O_3) as appropriate (J. B. Thompson, personal commun., 1975). Such $Al_2(Fe,Mg)_{-1}Si_{-1}$ reactions could displace projected bulk compositions in AKFM so that three-phase fields are replaced by two-phase tie lines (or even single phase regions) resulting in the disappearance or appearance of phases at constant X_{Mg}. Clearly, natural reactions will include the simultaneous operation of several exchange reactions in addition to $FeMg_{-1}$ and $Al_2(Fe,Mg)_{-1}Si_{-1}$.

NOTE ON THE REACTION BETWEEN DISCONTINUOUS REACTIONS AND END-MEMBER INVARIANT POINTS

The discontinuous ($FeMg_{-1}$) reactions terminate at the end-member invariant points (in KFASH or KMASH) *without metastable extension.* The location of discontinuous reactions relative to the stable and metastable univariant curves in the end-member systems is determined by the Schreinemakers labelling of absent phases (see Zen, 1966, for a discussion of notation) or by the relative X_{Mg} (and hence K_D) of participating phases. In some cases only metastable portions of discontinuous reactions may reach end-member invariant points, if they intersect other discontinuous ($FeMg_{-1}$) reactions elsewhere in P–T space (at constant aH_2O). The dashed portions of discontinuous reactions in the P–T diagrams for KFASH (in figs. 1 and 3) are not intended to imply metastable extensions but to facilitate construction of T–X(Fe–Mg) and P–X(Fe–Mg) sections relative to the P–T location of KFASH invariant points.

ACKNOWLEDGMENTS

The writer is grateful to the editors for permission to include some of the review aspects of this and the following paper. Discussions with James B. Thompson and other colleagues at Harvard contributed much to the development of this study. The facilities for the project were supported by grants from the National Science Foundation (#DES74-13673) and the Committee on Experimental Geology and Geophysics at Harvard. Critical reviews by Arden L. Albee, Charles V. Guidotti, Paul C. Hess, and Malcolm J. Rutherford significantly improved the manuscript.

REFERENCES

Albee, A. L., 1962, Relationships between the mineral association, chemical composition, and physical properties of the chlorite series: Am. Mineralogist, v. 47, p. 851-870.

———— 1965a, A petrogenetic grid for the Fe–Mg silicates of pelitic schists: Am. Jour. Sci., v. 263, p. 512-536.

———— 1965b, Phase equilibria in three assemblages of kyanite-zone pelitic schists, Lincoln Mountain Quadrangle, central Vermont: Jour. Petrology, v. 6, p. 246-301.

———— 1972, Metamorphism of pelitic schists: reaction relations of chloritoid and staurolite: Geol. Soc. America Bull., v. 83, p. 3249-3268.

Best, M. G., and Weiss, L. E., 1964, Mineralogical relations in some pelitic hornfelses from the southern Sierra Nevada, California: Am. Mineralogist, v. 49, p. 1240-1266.

Bowen, N. L., 1928, The evolution of the igneous rocks: New York, Dover Pubs., 334 p.

Chinner, G. A., 1965, The kyanite isograd in Glen Clova, Angus, Scotland: Mineralog. Mag., Tilley v. (34A), p. 132-143.

Dougan, T. W., 1974, Cordierite gneisses and associated lithologies of the Guri Area, northwest Guayana Shield, Venezuela: Contr. Mineralogy Petrology, v. 46, p. 169-188.

Evans, B. W., and Guidotti, C. V., 1966, The sillimanite–potash feldspar isograd in Western Maine, U.S.A.: Contr. Mineralogy Petrology, v. 12, p. 25-62.

Finger, L. W., and Burt, D. M., 1972, REACTION, a Fortran IV computer program to balance chemical reactions: Carnegie Inst. Washington Year Book 71, p. 616-622.

Grant, J. A., 1973, Phase equilibria in high-grade metamorphism and partial melting of pelitic rocks: Am. Jour. Sci., v. 273, p. 289-317.

Greenwood, H. J., 1967, The N-dimensional tie-line problem: Geochim. et Cosmochim. Acta, v. 31, p. 465-490.

———— 1975, Thermodynamically valid projections of extensive phase relationships: Am. Mineralogist, v. 60, p. 1-8.

Griffen, D. T., and Ribbe, P. H., 1973, The crystal chemistry of staurolite: Am. Jour. Sci., v. 273-A, p. 479-495.

Guidotti, C. V., 1970, The mineralogy and petrology of the transition from the lower to upper sillimanite zone in the Oquossoc Area, Maine: Jour. Petrology, v. 11, p. 277-336.

———— 1974, Transition from staurolite to sillimanite zone, Rangeley Quadrangle, Maine: Geol. Soc. America Bull., v. 85, p. 475-490.

Guidotti, C. V., Cheney, J. T., and Conatore, P., 1975, Coexisting cordierite + biotite + chlorite from the Rumford Quadrangle, Maine: Geology, v. 3, p. 147-148.

Hensen, B. J., 1971, Theoretical phase relations involving cordierite and garnet in the system MgO–FeO–Al_2O_3–SiO_2: Contr. Mineralogy Petrology, v. 33, p. 191-214.

Hess, P. C., 1969, The metamorphic paragenesis of cordierite in pelitic rocks: Contr. Mineralogy Petrology, v. 24, p. 191-207.

———— 1973, Figure 9, *in* Miyashiro, Akiho, Metamorphism and Metamorphic Belts: New York, Halsted Press, p. 81.

Hoschek, G., 1969, The stability of staurolite and chloritoid and their significance in metamorphism of pelitic rocks: Contr. Mineralogy Petrology, v. 22, p. 208-232.

Korzhinskii, D. S., 1959, Physicochemical basis of the analysis of the parageneses of minerals: New York, Consultants Bur., 142 p.

———— 1963, Extreme conditions and their significance in mineral systems, *in* Vinogradov, A. P., ed., Chemistry of the Earth's Crust, v. I, Vernadskii centenary: Moscow, Akad Nauk, SSSR, p. 62-86.

Osberg, P. H., 1971, An equilibrium model for Buchan-type metamorphic rocks, south-central Maine: Am. Mineralogist, v. 56, p. 569-576.

Ramberg, H., 1944, Petrological signicance of sub-solidus phase transitions in mixed crystals: Norsk geol. Tiddskr, v. 24, p. 42-73.

Reinhardt, E. W., 1968, Phase relations in cordierite-bearing gneisses from the Gananoque area, Ontario: Canadian Jour. Earth Sci., v. 5, p. 455-482.

Ricci, J. E., 1951, The phase rule and heterogeneous equilibrium: New York, Van Nostrand Co. (Dover Pubs. Inc. Reprint, 1966), 505 p.

Richardson, S. W., 1968, Staurolite stability in a part of the system Fe–Al–Si–O–H: Jour. Petrology, v. 9, p. 467-488.

Rumble, D., 1971, Chloritoid–staurolite quartzites from the Moosilauke Quadrangle, New Hampshire: Carnegie Inst. Washington Year Book 69, p. 290-294.

Schreyer, W., and Seifert, F., 1969, Compatibility relations of the aluminum silicates in the systems $MgO–Al_2O_3–SiO_2–H_2O$ and $K_2O–MgO–Al_2O_3–SiO_2–H_2O$ at high pressures: Am. Jour. Sci., v. 267, p. 371-388.

Seifert, F., 1970, Low-temperature compatibility relations of corderite in haplopelites of the systems $K_2O–MgO–Al_2O_3–SiO_2–H_2O$: Jour. Petrology, v. 11, p. 73-99.

Smith, J. V., 1968, The crystal structure of staurolite: Am. Mineralogist, v. 53, p. 1139-1155.

Tewhey, J. D., and Hess, P. C., 1974, Continuous metamorphic facies changes as related to chlorite disappearance in a contact metamorphic aureole: Geol. Soc. America Northeast Sec., Abs. with Programs, p. 80.

Thompson, A. B., 1974, Calculation of muscovite–paragonite–alkali feldspar phase relations: Contr. Mineralogy Petrology, v. 44, p. 173-194.

Thompson, J. B., Jr., 1957, The graphical analysis of mineral assemblages in pelitic schists: Am. Mineralogist, v. 42, p. 842-858.

———— 1961, Mineral facies in pelitic schists, *in* Sokolov, G. A., ed., Physicochemical problems in the formation of rocks and mineral deposits: Moscow, Akad. Nauk. SSSR, p. 313-325 [in Russian with English summary].

———— 1972, Oxides and sulfides in regional metamorphism of pelitic schists: Internat. Geol. Cong., 24th, Montreal, 1972, Proc., Sect. 10, p. 27-35.

Thompson, J. B., Jr., and Norton, S. A., 1968, Palaeozoic regional metamorphism in New England and adjacent areas, *in* Zen, E-an, ed., Studies of Appalachian Geology: Northern and Maritime: New York, Intersci., p. 319-327.

Thompson, J. B., Jr., and Thompson, A. B., in preparation, A model system for mineral facies in pelitic schists.

Tracy, R. J., Robinson, P. R., and Thompson, A. B., in press, Garnet composition and zoning in the determination of temperature and pressure of metamorphism, central Massachusetts: Am. Mineralogist, in press.

Weisbrod, A., 1973, Refinements of the equilibrium conditions of the reaction Fe cordierite + almandine + quartz + sillimanite ($+H_2O$): Carnegie Inst. Washington Year Book 72, p. 518-521.

Zen, E-an, 1966, Construction of pressure-temperature diagrams for multicomponent systems after the method of Schreinemakers—a geometric approach: U.S. Geol. Survey Bull. 1225, 56 p.